JOURNAL OF THERMOPHYSICS AND HEAT TRANSFER
Vol. 8, No. 3, July–Sept. 1994

Feasibility of Determining Haze Properties During High-Speed Titan Entry

H. F. Nelson*
University of Missouri—Rolla, Rolla, Missouri 65401

An international cooperative project between the National Aeronautics and Space Administration and the European Space Agency is planning to send a probe into the atmosphere of Titan (a moon of Saturn) as part of the Cassini Mission to Saturn. This article analyzes the feasibility of measuring the intensity of atomic carbon and hydrogen line emission in the shock layer during the high-velocity portion of the entry to determine the number density and composition of the organic haze particles in the Titan atmosphere. Analysis indicates that the line radiation signal-to-noise ratios are high enough so that determination of the haze particle number density and composition appears to be feasible. The analysis may be applicable to other future planetary missions.

Nomenclature

A_{ul} = Einstein coefficient for spontaneous emission, 1/s
C_p = particle specific heat, 1.80 kJ/(kg-K)
c = speed of light
D = particle diameter, mμ
d_0 = gas-molecule diameter, 6.0×10^{-10} m
E_u = energy of upper state, J
F_{1-2} = view-factor for radiometer
g_u = degeneracy of upper state of transition
H = enthalpy, kJ/kg
h = Planck's constant, J/K
I_λ = radiation emission, w/(cm^3-stradian)
K_{n_p} = Knudsen number of haze particle
k = Boltzmann's constant, J-s
L = particle vaporization energy, J/kg
L_0 = particle heat of evaporation, 360 kJ/kg
N = number density, 1/cm^3
P = gas pressure, Pa
$\dot{P}$ = particle flow rate, particles/(cm^2-s)
Q = total heat transfer, J
$\dot{Q}_c$ = convective heat transfer rate, W
$\dot{Q}_r$ = radiative heat transfer rate, W
$\dot{q}_c$ = convective flux to haze particle, W/cm^2
$\dot{q}_r$ = radiative flux to haze particle, W/cm^2
R = radius of view-cylinder, cm
S = photons emitted
$\dot{S}$ = photon emission rate, photons/s
T = temperature, K
T_v = vibrational temperature, K
T_{vap} = particle evaporation temperature, 300 K
t = time, s
t_v = particle evaporation time, s
V = velocity, m/s
$V_v\Omega$ = view-volume times solid angle, stradian-cm^3
V_0 = initial entry velocity, 6220 m/s
x = distance in front of window, cm
Z = electronic partition function
α_c, α_r = convective, radiative accommodation coefficient
Δ = depth-of-field for optics, 0.1 cm
δ^* = distance for particle to explode, cm
$\delta(t)$ = Dirac-delta function
δ_0 = shock wave standoff distance, cm
λ = wavelength, Å
ρ = density, kg/m^3
τ = time chop interval, s
σ = standard deviation of signal

Subscripts
g = shock layer gas
l = lower state of transition
p = haze particle
u = upper state of transition
∞ = freestream

Introduction

THE Cassini Mission[1–7] will explore Saturn and its system of rings and satellites as well as the atmosphere and surface of Titan. Titan is Saturn's largest moon and one of the few moons in the solar system with a substantial atmosphere. The atmosphere is opaque, with multiple layers of aerosols, ranging from thin smog-like hazes to thick clouds of frozen or liquid methane. The organic chemistry in Titan's atmosphere may resemble the chemistry in Earth's primitive atmosphere before life began; consequently, Titan is of high scientific interest.

The Cassini spacecraft includes a Saturn orbiter and a Titan atmospheric entry probe (Huygens probe). Launch is planned for the 1995–1997 time period. The spacecraft will be inserted into an orbit around Saturn. Subsequently, the probe will be separated from the spacecraft and it will enter and descend through Titan's atmosphere as shown schematically in Fig. 1. During the 2- to 3-min high-speed entry the probe descends to about 200 km and its velocity decreases to about 260 m/s.

Titan's atmosphere is composed mainly of molecular nitrogen, methane, hydrogen, and possibly argon, and a number of minor species containing H, C, and O. Table 1 gives the best estimate and uncertainty ranges at altitudes above 175 km where the composition is believed to be nearly uniform with altitude.[8] Note the large uncertainties for N_2 (65–98%), CH_4 (2–10%), and argon (0–25%). Yung et al.[9] performed a photochemical analysis of the atmosphere and concluded that the composition of the major species is nearly constant from about 50 to 850 km. They developed a model for atmospheric composition containing 97.2% N_2, 2% CH_4, and

Received June 30, 1993; presented as Paper 93-2762 at the AIAA 28th Thermophysics Conference, Orlando, FL, July 6–9, 1993; revision received Oct. 15, 1993; accepted for publication Oct. 19, 1993.

*Professor of Aerospace Engineering, Thermal Radiative Transfer Group, Department of Mechanical and Aerospace Engineering and Engineering Mechanics. Associate Fellow AIAA.

Table 1 Titan atmosphere at altitudes above 175 km

Atmospheric gases	Best estimate	Uncertainty range
N_2	0.90	0.65–0.98
CH_4	0.02	0.02–0.10
Ar	0.00	0.00–0.25
H_2	0.00	0.00–0.004
Atmospheric haze particles	**Best estimate**	**Uncertainty range**
Column density, g/cm^2	4×10^{-6}	$2.0–4.0 \times 10^{-6}$
Diameter, μm	0.60	0.10–1.0
Number density, 1/cm^3	0.20	—
Particle density, g/cm^3	1.80	1.0–1.8
Particle composition	H-C	H-C-N-O

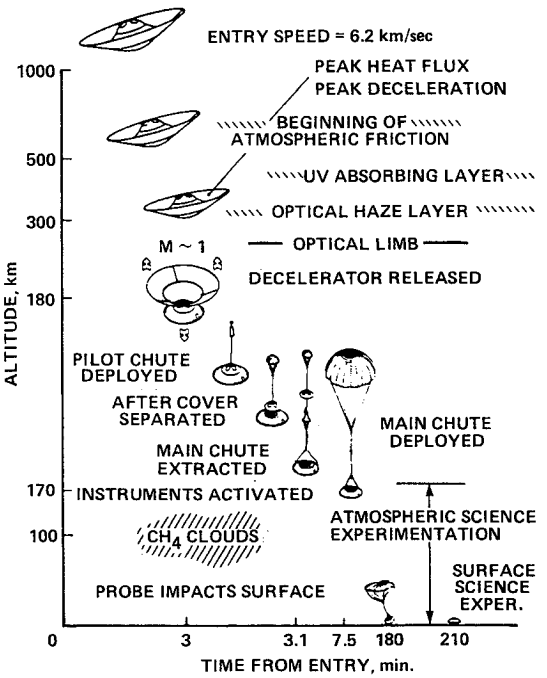

Fig. 1 Schematic diagram of the Titan probe atmospheric entry.

0.2% H_2. The current model for altitude variation of density and temperature for Titan was developed by Lellouch and Hunten.[10]

Nelson et al.[11] have shown that shock layer radiation from the CN(violet) bands can be used to determine mole fractions of the three major gases in the atmosphere (N_2, CH_4, and argon) to about ± 0.015 for N_2, ± 0.003 for CH_4, and ± 0.01 for argon over altitudes from about 350 to 250 km. This is much better than the present uncertainties in the composition given in Table 1. The objective of this article is to show that the atmospheric haze number density and composition can be determined by measuring emission of the hydrogen $L\alpha$ line at 1216 Å, and the atomic carbon line at 2478 Å.

Titan Atmospheric Haze

Titan's atmosphere contains a thick, orange haze at altitudes above about 150 km.[4] The atmospheric haze appears to consist of three components: 1) a photochemical aerosol haze in the stratosphere between altitudes of 50–500 km, 2) a mixture of condensed hydrocarbons (CHs) and nitriles (CNs) in the lower atmosphere, 50- to 80-km altitude, and 3) methane clouds between 10 and 35 km.[12] The high-speed portion of Titan entry passes through most of the atmospheric haze layers.

Rages and Pollack[13] used Voyager radiation measurements and the assumption of spherical particles to determine that 1) the mean haze particle diameter is between 0.40–0.70 μm, and 2) the haze particle number density was about 0.2 particles/cm^3. The haze appears to be uniformly distributed throughout the entire atmosphere at altitudes from 300 to 350 km. Thompson and Sagan[14] determined the haze layer column density to be $4.0 \pm 2.0 \times 10^{-6}$ g/cm^2 for altitudes above 175 km. Optical properties of synthesized haze particles (called tholin), have been measured by Khare et al.[15] Tholin was found to contain more than 100 different organic compounds, mainly complex, high-order hydrocarbons.[16,17]

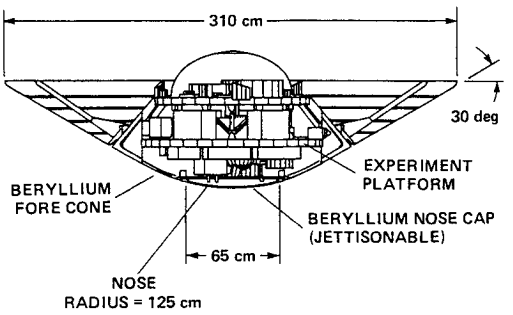

Fig. 2 Titan probe with its decelerator extended.

Hugyens Probe Configuration

The Hugyens probe is described in the Cassini phase A study.[7] Figure 2 presents a schematic drawing of the configuration. The forebody is a spherical blunted cone with a nose radius of 1.25 m when the decelerator is fully deployed. In this configuration the probe mass is 192 kg and its ballistic coefficient is 20.2 kg/m^2.

Trajectory

The atmospheric entry trajectory considered in this study is a vertical flight path (entry angle of -90 deg) with an entry velocity of 6220 m/s at 1000-km altitude. Table 2 gives specific trajectory data at 6-s intervals over the altitude range from about 400 to 200 km where significant optical radiation is emitted in the shock layer.

Shock Layer Analysis

The shock layer composition and radiation were calculated using the one-dimensional, nonequilibrium computer code, Stagnation Point RAdiation Program (SPRAP), which was developed for shock waves in air.[18–20] It has been shown to give good results when compared to Earth entry and shock tube experimental data taken under nonequilibrium conditions. A two-temperature model (T-T_v model) is used in the chemistry portion of the code. In the present work the code was modified for the Titan atmosphere to include carbon, hydrogen, and noble gas species.[11]

Typical shock layer calculations are shown in Figs. 3 and 4. These figures are for a gas mixture with a N_2/CH_4 ratio of 98/2 and 0% argon, which is very close to Yung's model atmospheric composition.[9] Species mole fractions are plotted in Fig. 3 as a function of distance behind the shock wave for the trajectory point at 118 s after the 1000-km entry point (see Table 2). For this case, $\delta_0 = 11.3$ cm. This figure also shows the mole fractions that would result if the shock layer was in thermodynamic equilibrium. These values are denoted by the dashed curves that connect with the right vertical axis labeled ∞.

All the diatomic molecules that form in the shock layer (CN, H_2, CH, NH, and C_2) overshoot their equilibrium values very near the shock wave, but only CN and C_2 maintain these values across most of the shock layer. The CN concentration in the shock layer is almost linearly proportional to the amount of CH_4 in the atmosphere for small amounts of CH_4. The mole fraction of CN is about a factor of 5 higher than its equilibrium value over most of the shock layer, which indicates that nonequilibrium CN radiation is enhanced over its equilibrium value. CH_4 is not shown in Fig. 3, because it

Table 2 Atmospheric entry conditions for nominal Titan atmosphere V_0 = 6220 m/s, −90-deg entry

Time, s	Altitude, km	V_∞, m/s	ρ_∞, kg/m^3	P_∞, Pa	T_∞, K	δ_0, cm
94	413.5	6122	0.0000201	1.13	187	13.1
100	377.2	5973	0.0000390	2.19	187	12.1
106	342.1	5699	0.0000758	4.23	186	11.9
112	309.2	5231	0.0001450	8.00	185	12.3
118	279.8	4535	0.0002620	14.37	183	11.3
124	255.1	3678	0.0004440	24.03	181	12.0
130	235.6	2825	0.0006760	36.29	179	13.3

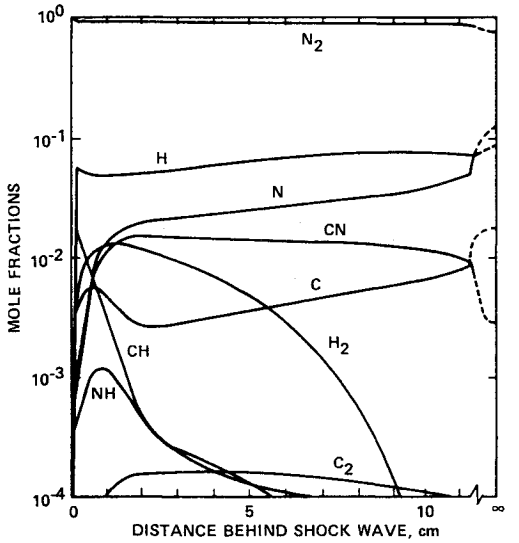

Fig. 3 Species mole fraction as a function of position in the Titan probe shock layer for entry time of 118 s. Atmosphere is 98% N_2, 2% CH_4 by volume.

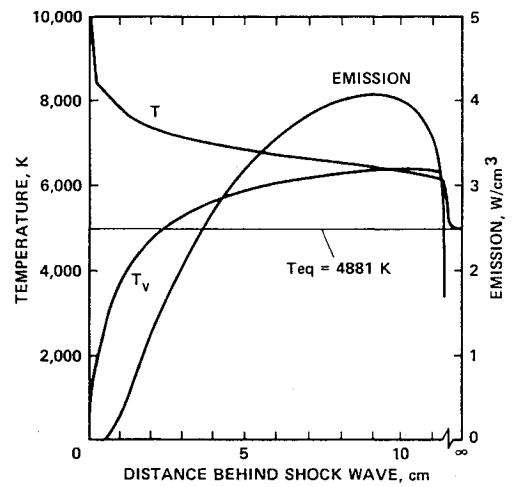

Fig. 4 Temperatures and spontaneous emission from CN(violet) and CN(red) vs position in the Titan probe shock layer for entry time of 118 s. Atmosphere is 98% N_2, 2% CH_4 by volume.

dissociates very quickly. This effect is evident in the fast rise in the mole fractions for species containing C and H atoms just behind the shock wave. Mole fractions of C and H atoms tend to be relatively constant across the shock layer and slightly below their equilibrium values. This trend will be used in the haze particle analysis.

Temperatures T and T_v and the total spontaneous emission (W/cm^3) from CN(violet) and CN(red), into 4π sr and integrated over the spectral band from 2000 to 20,000 Å, are shown in Fig. 4 for the trajectory point at 118 s. T and T_v are significantly different over most of the shock layer. The heavy particle translational-rotational temperature T decreases as

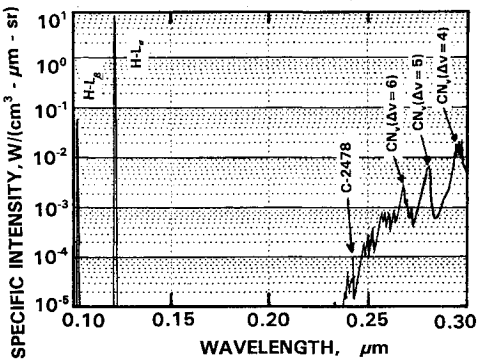

Fig. 5 Spontaneous emission from a nonequilibrium shock layer near its maximum emission point in the shock layer for entry time of 118 s. Atmosphere is 98% N_2, 2% CH_4 by volume.

energy is transferred into the vibrational and electronic modes which causes the vibrational-electronic-electron temperature T_v to increase. Both T and T_v are higher than the equilibrium temperature of 4881 K across most of the shock layer. Thus, not only will nonequilibrium CN radiation be enhanced due to high CN population, but also because the electronic temperature is higher than the equilibrium value. This effect is evident in Fig. 4 by the increasing magnitude of CN emission across the shock layer as the electronic temperature increases, even though CN concentration is nearly constant.

The spectral distribution of spontaneous emission at a point in the shock layer near the maximum value of emission (≈9.5 cm behind the shock wave) is shown in Fig. 5 for wavelengths from 1000 to 3000 Å. The atomic hydrogen $L\alpha$ and $L\beta$ lines are easily identified near 1200 Å. The atomic carbon line at 2478 Å is harder to identify because of the CN(violet) band structure.

Haze Shock Layer Particle Analysis

Table 1 summarizes the best estimates of several haze particle properties and gives an estimate of their uncertainty. The properties of the haze particles are very uncertain. It seems reasonable to try to reduce these uncertainties.

In order to determine the feasibility of using shock layer radiometer measurements to determine haze number density and composition as a function of altitude, several assumptions are necessary:

1) All calculations are done along the stagnation streamline.

2) Haze particles are spherical and sparsely distributed in the atmosphere.

3) Haze particle number density is small, so it does not influence the shock layer thermodynamic state.

4) Haze particles are not affected by passing through the shock wave.

5) The shock layer has constant thermodynamic properties and composition along its stagnation streamline which are representative of the specific time (altitude) along the trajectory.

6) The shock layer is optically thin in the spectral bands of interest for the haze analysis.

7) The particles are composed of C_6H_{12} molecules as a representative high-order hydrocarbon.

8) The particle flow time across the shock layer is approximately δ_0/V_∞.

9) The particles explode in the shock layer, or when they hit the radiometer window.

10) During an explosion the C and H atoms from the particles instantly equilibrate with the surrounding gas-atoms and gas-molecules.

11) During an explosion a detectable spike will occur in the shock layer emission due to the increased number of C and H atoms.

12) The number of spikes/s is proportional to the particle number density, and the magnitude of the spikes is proportional to the number of radiating atoms from the particles.

13) The population of the excited electronic states of the C and H atoms is determined from the vibrational temperature in the shock layer.

Concept

The haze radiometer experiment relies on the measurement of the emission of radiation from the C and H atoms released when the haze particles explode. The radiation is detected from a cylindrical volume centered on the probe stagnation streamline at the probe stagnation point as shown schematically in Fig. 6. Radiative emission from each explosion event is collected by optics behind a window at the probe stagnation point. The collection optics are arranged so that only radiation emitted in the cylindrical volume at the optical focal point is detected. The intensity of the emitted radiation is integrated over small time intervals τ to obtain a signal that is a measure of the total radiative energy emitted during the interval. This includes radiation from the shock layer gas-atoms and from the particle-atoms. Radiation from the shock layer gas-atoms and the particle-atoms can be separated by signal analysis. The radiation is detected in two small spectral bands located on the atomic hydrogen $L\alpha$ line and on the atomic carbon line at 2478 Å. Consequently, the signal is linearly proportional to the number density of atomic hydrogen and/or atomic carbon.

Haze Particle Statistics

The haze particle is assumed to have $D = 0.6\ \mu$m,[13] which yields a volume ($\pi D^3/6$) of $36\pi \times 10^{-15}$ cm^3. The particle density is 1.8 g/cm^3 (Ref. 21, p. 216), so the particle mass is $64.8\pi \times 10^{-15}$ g. The mass of a C_6H_{12} molecule is 1.39×10^{-22} g; thus, there are 1.46×10^9 C_6H_{12} molecules in a typical haze particle. This yields 8.76×10^9 C atoms and 1.75×10^{10} H atoms per haze particle. If the number of atoms is calculated per volume instead of per mass, assuming a C_6H_{12} molecule diameter of 6 Å (Ref. 22, p. 53), the volume of a C_6H_{12} molecule is $36\pi \times 10^{-24}$ cm^3, and the number of C_6H_{12} molecules per particle is 1.0×10^9. Therefore, there are 6×10^9 C atoms and 12×10^9 H atoms per particle. Thus, both the mass and volume analyses yield similar results. In this study the mass analysis is used.

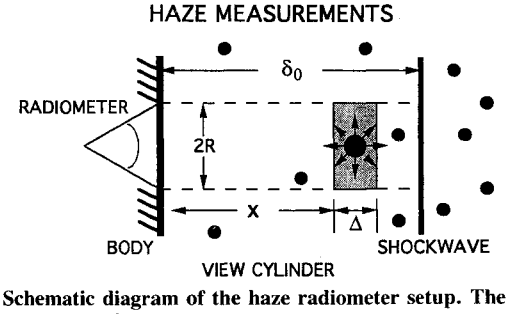

Fig. 6 Schematic diagram of the haze radiometer setup. The shock standoff distance is δ_0.

Shock layer calculations were made for the nominal atmospheric composition at entry times from 94 to 130 s, or altitudes from 413 to 235 km, to determine the feasibility of measuring the number density and composition of the haze particles. A summary of the shock layer conditions used in the haze analysis is given in Table 3.

Figure 7 shows the number of haze particles that cross the shock and enter the cylindrical view-volume as a function of time along the trajectory and the view-volume radius. The number of particle explosions that are detected per second can be controlled by varying the radius of the field-of-view. For $R = 0.1$ cm, about 4000 to 2000 particles enter the field-of-view per second, which implies approximately 0.0003 to 0.0005 s between particle explosions.

Particle Vaporization Time

Particle vaporization time is dependent on the flow surrounding the particle. The Knudsen number for the particles in the shock layer is $K_{n_p} = kT/(2\sqrt{\pi} d_0^2 PD)$.[23] When K_{n_p} is greater than 1, the particle is in a free molecule flow regime. K_{n_p} is calculated assuming that the shock layer in mainly N_2 ($d_0 = 6.0 \times 10^{-10}$ m), and that the particles have $D = 0.6$ μm. Table 4 gives the value of K_{n_p} along the trajectory. Clearly, the particles are in a free molecule flow.

The particles enter the shock layer at V_∞ with $N_p = 0.2$ particles/cm^3. The gas on the other hand is slowed down as it crosses the shock wave to about $V_\infty/10$. Thus, the number of gas-molecules that hit the particle per second is $0.9V_\infty N_g \pi D^2/4$, where $0.9V_\infty$ is the relative velocity difference between the particle and the gas, and N_g is the gas-molecule number density. The energy per gas-molecule is estimated from energy conservation across the shock wave; thus, $H_\infty + V_\infty^2/2 = H_g + V_g^2/2$. In the freestream $V_\infty^2/2 >> H_\infty$, and in the shock layer $H_g >> V_g^2/2$, so the energy per unit mass in the shock layer is $H_g = V_\infty^2/2$. Each gas molecule has mass m_g, so the energy per gas molecule is $m_g V_\infty^2/2$. The efficiency in transferring this amount of energy to the particle during a collision is given by the accommodation coefficient α_c. Consequently, the rate at which energy is convected from the gas to the haze particles is $\alpha_c(9V_\infty N_g \pi D^2/40)(m_g V_\infty^2/2)$, J/s. Since $m_g N_g = \rho_g$ (shock layer gas density), the approximate haze particle convective heating rate (W) is

$$\dot{Q}_c = 9\alpha_c \rho_g \pi D^2 V_\infty^3/80 \tag{1}$$

The particle radiative heating rate per unit area is assumed to be equal to the vehicle stagnation point heating rate. These values are taken from Ref. 11 and given in Table 4. Consequently, the haze particle radiative heating rate is

$$\dot{Q}_r = \alpha_r \dot{q}_r \pi D^2 \tag{2}$$

where α_r is the radiation accommodation coefficient.

The energy required to vaporize a liquid haze particle is

$$L = C_p(T_{\text{vap}} - T_\infty) + L_0 \tag{3}$$

in J/kg, where T_∞ is the particle temperature as it enters the shock layer. The haze particle properties are estimated assuming they are composed of C_6H_{12} molecules. L_0 is assumed to be 360 kJ/kg (85.6 cal/g, see Ref. 22, p. 130 for cyclohexane). C_p is taken as 1.80 kJ/(kg-K) from Ref. 24. The vaporization temperature for C_6H_{12} is a function of pressure. T_{vap} is assumed to be 300 K (Ref. 22, p. 159). T_{vap} increases as pressure increases. The shock layer pressures given in Table 3 indicate that this value of T_{vap} may be slightly high. Assuming T_∞ is 185 K yields $L = 1.80(300 - 185) + 360 = 567$ kJ/kg. The energy required to vaporize an organic haze particle is

$$Q = \rho_p L \pi D^3/6 \tag{4}$$

Table 3 Shock layer conditions

Time, s	T, K	T_v, K	P, Pa	ρ, kg/m^3	N_C,[a] 1/cm^3	N_H,[a] 1/cm^3
94	13,000	7,600	733	0.00027	2.04	27.0
100	10,000	7,600	1,380	0.00040	4.53	58.1
106	9,300	8,100	2,251	0.00070	10.2	111.0
112	8,500	7,700	3,603	0.00127	13.4	212.0
118	7,000	5,900	4,866	0.00159	18.9	327.0
124	5,000	2,500	5,200	0.00328	43.7	298.0
130	3,680	1,350	4,494	0.00406	0.007	42.9

[a]Multiplied by 10^{-13}.

Table 4 Shock layer parameters $\alpha_c = \alpha_r = 1$

Time, s	$\dot{P}$, particles/(cm^2-s)	δ^*, cm	K_{np}	$\dot{q}_c$, W/cm^2	$\dot{q}_r$, W/cm^2
94	122,485	8.96	319	2,788	0.60
100	119,430	6.34	131	3,836	2.11
106	113,955	3.98	74.5	5,831	6.32
112	104,660	2.60	42.5	8,180	10.64
118	90,655	2.75	25.9	6,673	16.24
124	73,595	2.04	17.3	7,344	3.16
130	56,530	2.80	14.8	4,119	0.70

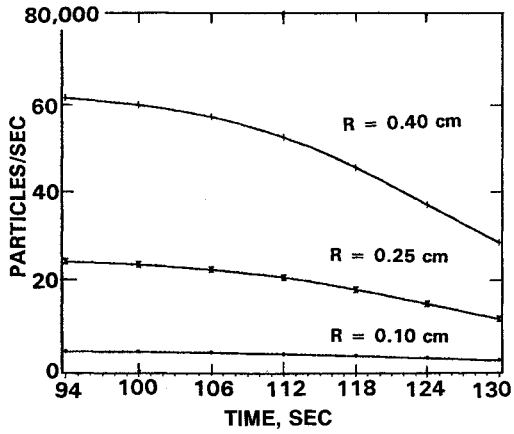

Fig. 7 Haze particles crossing the shock wave as a function of time along the trajectory.

in units of joules per particle, where the nominal density of an organic haze particle is $\rho_p = 1800$ kg/m^3 (Ref. 21, p. 216).

The time required for the gas-molecules to transfer energy equal to the vaporization energy to the haze particle is obtained from Eqs. (1), (2), and (4) as $t_v(\dot{Q}_c + \dot{Q}_r) = Q$, so that

$$t_v = \rho_p LD/[6(\alpha_r \dot{q}_r + 9\alpha_c \rho_g V_\infty^3/80)] \tag{5}$$

Calculations show that the radiative contribution to t_v is negligible compared to the convective contribution. Note that t_v will be sensitive to the value of α_c.

Drag on the organic haze particle is estimated from Newton's second law as

$$\frac{d}{dt}[\rho_p \pi (D^3/6)(V_p - V_g)] = -P\pi D^2/4 \tag{6}$$

If the particle does not vaporize as it moves across the shock layer, D remains constant, and one has

$$\frac{d}{dt}(V_p - V_g) = \frac{-3P}{2\rho_p D} \tag{7}$$

and integrating this across the shock layer yields

$$V_p - V_g = \frac{-3Pt}{2\rho_p D} + 0.9V_\infty \tag{8}$$

where $V_p - V_g$ is assumed to be $0.9V_\infty$ at $t = 0$. Using data from Table 3, the values of $(3Pt/2\rho_p D)$ are 115, 151, and 308 m/s, respectively, at the entry points corresponding to 94, 118, and 130 s. These values are clearly negligible compared to $0.9V_\infty$; consequently, particle drag is negligible.

Now it is possible to estimate the distance the particle travels in the shock layer prior to obtaining its required vaporization energy. Since drag is negligible, the particle moves at constant velocity V_∞ in the shock layer. The distance traveled when the particle has absorbed its vaporization energy is $\delta^* = V_\infty t_v$. These distances are tabulated in Table 4 for $\alpha_c = \alpha_r = 1$. Since δ_0 is 11–13 cm (Table 3), almost all of the particles will impact the radiometer window for reasonable values of α_c and α_r ($\approx$0.2). This impact will cause them to fragment and radiate.[25,26]

Haze Particle Radiation

The emission of atomic line radiation is directly proportional to the atom number density

$$I_\lambda = N_u A_{ul} hc/(4\pi\lambda) \tag{9}$$

where I_λ is the line emission, and N_u is the number density of the upper state of the emission transition. Emission from the gas- and particle-atoms is given by the same relationship; however, the value of N_u is different, because it represents either gas-atom, or particle-atom number density. The gas emission is relativity steady, so when a particle explodes the emission will suddenly increase due to the additional radiating atoms (increase in N_u). The ratio of the population of the atom upper state to the total atom population is

$$N_u/N = g_u \exp[-E_u/(kT_v)]/Z \tag{10}$$

where Z is evaluated at T_v, and N is the number density of the atom at the specific point of interest in the shock layer. N_u is a strong function of the electronic temperature T_v. Values of N_C and N_H are given in Table 3 for entry times from 94 to 130 s.

Signal-to-Noise Ratio

The Titan haze particles are thought to be uniformly distributed throughout the atmosphere at altitudes between about 175–500 km. Thus, the radiometer instrument system should be designed to operate over most of this altitude range to obtain altitude resolution of the haze particle number density

and composition. A measurement uncertainty of less than 1% should insure adequate resolution of the haze distribution and evaluate the feasibility of the measurements.

The uncertainty of an optical measurement is usually characterized by its overall signal-to-noise ratio (SNR). The SNR for this experiment is evaluated by measuring the photon emission rate and then integrating this rate over short, consecutive time periods to calculate the average number of photons detected in a given time interval. This forms a set of repeated independent measurements of a random variable.

Since the photon energy is hc/λ, the number of photons emitted per second in volume V_v and solid angle Ω in the detector field-of-view is

$$\dot{S} = I_\lambda V_v \Omega \lambda/(hc) \tag{11}$$

The radiometer optics are assumed to view a constant diameter cylinder centered on the stagnation streamline and extending across the shock layer. It is assumed that the optics are such that the detector is focused on a plane of thickness Δ, located a distance x in front of the radiometer window as shown in Fig. 6. The equation for the volume times the solid angle is

$$V_v\Omega = (2\pi F_{1-2})(\pi R^2 \Delta) \tag{12}$$

where F_{1-2} is the view-factor between the detector window and the focal plane, and the shock layer is assumed to be optically thin. The value of F_{1-2} for this geometry is taken from Ref. 27, p. 826, configuration number 21. This yields

$$V_v\Omega = \pi^2(2R^2 + x^2 - x\sqrt{x^2 + 4R^2})\Delta \tag{13}$$

When the focal plane is at the window ($x \approx 0$), $V_v\Omega = 2\pi^2R^2\Delta$ and when the focal point is far from the window ($x \approx \infty$) $V_v\Omega = 2\pi^2R^4\Delta/x^2$. Note that $V_v\Omega$ is a function of 1) the distance to the optical focal plane, 2) the thickness of the optical focal plane, and 3) the cylinder diameter.

The number of emitted photons in the C and H lines are counted continuously during the entry as shown schematically in Fig. 8. The shock layer gas-atoms emit $\dot{S}_g$, and the particle-atoms emit $\dot{S}_p$ photons/s, the difference being due to the number densities of the gas- and particle-atoms. It is assumed that the particles explode with equal probability anywhere in the detector field-of-view. Integrating the photon emission rate over a short time interval τ, as shown schematically in Fig. 8, yields a set of repeated independent measurements of a random variable (number of photons in τ). This set of measurements obeys Poisson statistics if the number of photons in τ is large (1000, or more).[28] The mean, or average number of photons is

$$S_g = \dot{S}_g \tau \tag{14}$$

where, most of the τ have no particle explosions in them. For Poisson statistics, the mean and variance are equal. Thus, the noise, which is equal to the standard deviation, is $\sigma = \sqrt{S_g}$. The signal due to the particle-atoms is S_p, which formally can be expressed as

$$S_p = \int_0^\tau \dot{S}_p \delta(t)\, dt \tag{15}$$

It is assumed that the particle instantly achieves equilibrium with the surrounding gas and emits a spike of radiation as it explodes. Thus, the SNR is the ratio of the spike-like particle emission to the magnitude of the fluctuations in the S_g, so

$$\text{SNR} = S_p/\sigma \tag{16}$$

The statistical SNR analysis compares S_p to σ. The τ used to analyze the radiometer data must be large compared to the time for a particle to explode, but yet be small compared to the time between successive explosions so that most of the time intervals have no particle explosions in them. The time between explosions is related to the rate at which particles enter the shock layer, and it is controlled by the radius of the radiometer field-of-view. Figure 7 shows the rate to be roughly 1000–5000 particles per second, which corresponds to 0.001 to 0.0002 s between explosions, depending on the field-of-view radius, and the probe altitude and velocity.

Figures 9 and 10 show the values of the SNR (in dB) as a function of altitude for the carbon and hydrogen, respectively. Each figure shows SNR divided by the diameter of the radiometer field-of-view. Results are given for $\tau = 10^{-4}$, 10^{-5}, and 10^{-6} s; although, $\tau = 10^{-4}$ s is a little large for realistic applications. SNR values are shown for the particle exploding on the window and 6 cm in front of the window. Good SNR values are usually assumed to be larger than 40 dB, but SNR values as low as 20 dB are acceptable in some cases. The SNR for both the hydrogen and carbon atoms is large for altitudes between 450–280 km, so that this analysis implies that measurement of the emission in the atomic lines is a viable way to measure haze properties. SNR values predicted in this analysis will be reduced somewhat in real situations; however,

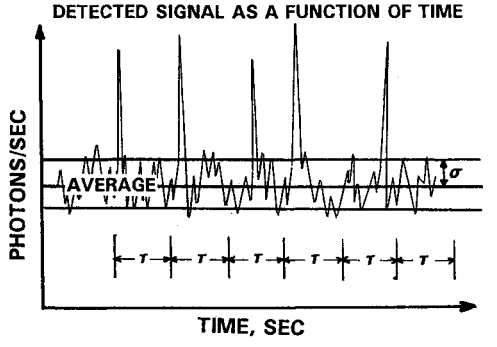

Fig. 8 Schematic diagram of the detected radiation as a function of time.

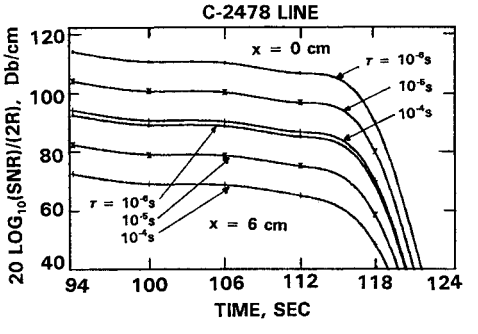

Fig. 9 SNR divided by view-cylinder diameter for the carbon 2478.56 line for particle explosion at window and 6 cm in front of window.

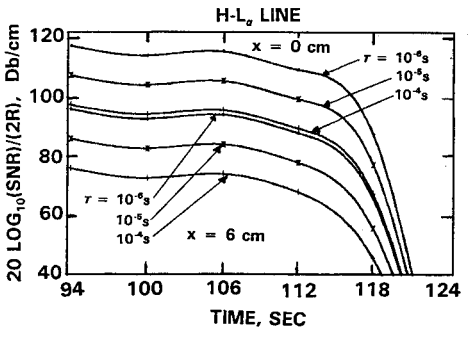

Fig. 10 SNR divided by view-cylinder diameter for the hydrogen 1215.67 line for particle explosion at window and 6 cm in front of window.

there appears to be ample signal strength to yield accurate analysis. An optimum design has not been attempted at this time.

There are three important points of the analysis:

1) The number of "spikes" is equal to the number of particle explosions. This number should be consistent for both the carbon and hydrogen line data. In reality, there are two detectors measuring the same phenomena, so accuracy should be easily maintained.

2) The magnitude of the emission spikes is directly related to the number of particle-atoms. Thus, the data will allow a determination of the particle composition.

3) If there is a need to investigate the particle composition further, one might also measure emission from atomic N and O lines. This would cover a range of possible particle compositions.

The lines used in this conceptual study may not be optimum. The C and H line radiation may be optically thick in the line center, where the analysis is undertaken; however, it is possible to move the detected band slightly away from the line center and still use the same analysis. The shock layer spectra is optically thin in the regions surrounding both atomic lines used in this analysis. Further analysis may determine that other lines are better suited for radiometer measurements. Also, the measurements may involve several lines, depending on the availability of radiometer channels. There may be problems with detectors and windows at these low wavelengths. One may have to use lithium-fluoride windows, or window-less detectors. Further study will address these situations.

The time chopper will blackout small time intervals with each chop. This blackout time can easily be accounted for in the statistics for counting the particles. Chopping at 10^5 or 10^6 chops/s, and storing and returning the data from a spacecraft, may require some creative design.

When the particles hit the window, it is assumed that they explode in a time interval equal to D/V_∞, which is the time interval between the front and rear of the particle hitting the window. This time is large compared to a Dirac-delta function, but small compared to τ and should not significantly influence the analysis. Particles impacting the window may pit the window, causing the window and the optics to deteriorate.[29] In this case an impact sensor can be used to count particles. These situations have not been investigated at present.

Summary and Conclusions

The Huygens Probe, which is a part of the Cassini mission to Saturn, offers an opportunity to determine the mole fractions of the major atmospheric species (N_2, CH_4, and argon), and the number density and composition of the haze particles in the Titan atmosphere from shock layer radiometer measurements during the high velocity portion of the entry between about 200- and 500-km altitude. The concept for determining the atmospheric composition from shock layer radiometer measurements was demonstrated by the PAET Earth atmosphere probe,[30] and shown to be feasible for Titan in Ref. 11.

The determination of the haze number density and composition as a function of altitude appears to be feasible; although, it is more risky than the gaseous atmospheric composition determination. It is a new concept, therefore, it has not been demonstrated in a realistic situation. The analysis is based on some critical assumptions like the size of the particles, the estimated particle composition, the explosion of the particles, and the "instant" equilibrium of the particle-atoms with the neighboring shock layer species, and the discrimination of the particle signals from the much stronger gas signals. The vaporization time is sensitive to the convective heating accommodation coefficient. If α_c is close to 1, the particle has a high probability of vaporizing in the shock layer rather than on the radiometer window. This will tend to decrease SNR, but it can be compensated for by enlarging the radiometer view-volume.

This analysis shows that haze composition and number density can be determined using two radiometer channels, one on the atomic hydrogen $L\alpha$ line at 1216 Å, and one on the 2478 Å line of atomic carbon. Dedicating additional channels to other lines of H and C and other possible haze particle-atoms (possibly N and O), additional information can be obtained.

The shock layer radiometer experiment appears to be feasible. It provides a direct measurement of atmospheric composition and haze number density and composition at altitudes above 170 km. In addition, a radiometer is simple, reliable, rugged, and relatively inexpensive.

Acknowledgments

This work was partly supported by IPA Assignment Agreement RT-0076/T-7932 between the University of Missouri—Rolla and NASA Ames Research Center. The author thanks Ellis E. Whiting of Eloret Institute, Sunnyvale, CA; and Chul Park, Roger A. Craig, and William C. Davy of the NASA Ames Research Center for their encouragement of this work.

References

[1]Gautier, D., and Ip, W. H., "Project Cassini: A Saturn Orbiter/Titan Probe Mission Proposal," *Origins of Life*, Vol. 14, 1984, pp. 801–807.

[2]Raulin, F., Gautier, D., and Ip, W. H., "Exobiology and the Solar System: The Cassini Mission to Titan," *Origins of Life*, Vol. 14, 1984, pp. 817–824.

[3]Scoon, G. E. N., and Flury, W., "Cassini Mission—The Titan Probe," International Astronautical Federation Paper 87-445, Oct. 1987.

[4]Swenson, B. L., Mascy, A. C., and Edsinger, L. E., "A New System Concept for a Titan Atmospheric Probe," AIAA Paper 84-0456, Jan. 1984.

[5]Swenson, B. L., "Titan Atmospheric Probe," *Journal of the British Interplanetary Society*, Vol. 37, 1984, pp. 366–369.

[6]Sergeyevsky, A. B., Courage, S. J., and Stetson, D. S., "Cassini—A Mission to the Saturnian System," American Astronomical Society Paper 87-423, Aug. 1986.

[7]Gautier, D., Ip, W., and Owen, T., "Cassini, Saturn Orbitor and Titan Probe: Report on the Phase A Study," European Space Agency, SCI(88)5, Oct. 1988.

[8]Hunten, D. M., Tomasko, M. G., Flasar, F. M., Samuelson, R. E., Strobel, D. F., and Stevenson, D. J., "Titan," *Saturn*, edited by T. Gehrels and M. S. Matthews, Univ. of Arizona Press, Tucson, AZ, 1984, pp. 671–759.

[9]Yung, Y. L., Allen, M., and Pinto, J. P., "Photochemistry of the Atmosphere of Titan: Comparison Between Model and Observations," *The Astrophysical Journal Supplement Series*, Vol. 55, July 1984, pp. 465–506.

[10]Lellouch, E., and Hunten, D. E., "Titan Atmospheric Engineering Model," European Space Agency Rept., ESLAB 87/199, Oct. 1987.

[11]Nelson, H. F., Park, C., and Whiting, E. E., "Titan Atmospheric Composition by Hypervelocity Shock Layer Analysis," *Journal of Thermophysics and Heat Transfer*, Vol. 5, No. 2, 1991, pp. 157–165.

[12]Samuelson, R. E., "Clouds and Aerosols of Titan's Atmosphere," *The Atmospheres of Saturn and Titan, Proceedings of an International Workshop* (Alpbach, Austria), European Space Agency Rept., ESA SP-241, 1985, pp. 99–197.

[13]Rages, K., and Pollack, J. B., "Vertical Distribution of Scattering Hazes in Titan's Upper Atmosphere," *ICARUS*, Vol. 55, pp. 50–62.

[14]Thompson, W. R., and Sagan, C., "Titan: Far-Infrared and Microwave Remote Sensing of Methane Clouds and Organic Haze," *ICARUS*, Vol. 60, 1984, pp. 236–259.

[15]Khare, B. N., Sagan, C., Arakawa, E. T., Suits, F., Callcott, T. A., and Williams, M. W., "Optical Constants of Organic Tholins Produced in a Simulated Titanian Atmosphere from Soft X-Ray to Microwave Frequencies," *ICARUS*, Vol. 60, 1984, pp. 127–137.

[16]Khare, B. N., Sagan, C., Zumberge, J. E., Sklarew, D. S., and Nagy, B., "Organic Solids Produced by Electrical Discharge in Re-

ducing Atmospheres: Tholin Molecular Analysis," *ICARUS*, Vol. 48, 1981, pp. 290–297.

[17]Khare, B. N., et al., "The Organic Aerosols of Titan," *Advances in Space Research*, Vol. 4, No. 12, 1984, pp. 59–68.

[18]Park, C., "Assessment of a Two-Temperature Kinetic Model for Dissociating and Weakly Ionizing Nitrogen," *Journal of Thermophysics and Heat Transfer*, Vol. 2, No. 1, 1988, pp. 8–16.

[19]Park, C., "Calculation of Nonequilibrium Radiation in the Flight Regimes of Aeroassisted Orbital Transfer Vehicles," *Thermal Design of Aeroassisted Orbital Transfer Vehicles*, edited by H. F. Nelson, Vol. 96, Progress in Astronautics and Aeronautics, AIAA, New York, 1985, pp. 395–418.

[20]Park, C., "Problems of Rate Chemistry in Flight Regimes of Aeroassisted Orbital Transfer Vehicles," *Thermal Design of Aeroassisted Orbital Transfer Vehicles*, edited by H. F. Nelson, Vol. 96, Progress in Astronautics and Aeronautics, AIAA, New York, 1985, pp. 515–537.

[21]Thompson, W. R., "A Physical and Chemical Study of Titan: Atmosphere, Clouds, and Haze," Ph.D. Dissertation, Cornell Univ., Ithaca, NY, 1984, p. 216.

[22]Kanury, A. M., *Introduction to Combustion Phenomena*, Gordon and Breach, New York, 1984.

[23]Vincenti, W. G., and Kruger, C. H., Jr., *Introduction to Physical Gas Dynamics*, Wiley, New York, 1965.

[24]Wark, K., *Thermodynamics*, 3rd ed., McGraw-Hill, New York, 1977, p. 831, Table A-19M.

[25]Eichorn, G., "Analysis of the Hypervelocity Impact Process from Impact Flash Measurements," *Space and Planetary Science*, Vol. 24, 1976, pp. 771–781.

[26]Jean, B., and Rollins, T. L., "Radiation from Hypervelocity Impact Generated Plasma," *AIAA Journal*, Vol. 8, No. 10, 1970, pp. 1742–1748.

[27]Siegel, R., and Howell, J. R., *Thermal Radiation Heat Transfer*, 2nd ed., Hemisphere, New York, 1981.

[28]Parzen, E., *Modern Probability Theory and Its Applications*, Wiley, New York, 1960, Chap. 8.

[29]Papadopoulos, P., Tauber, M. E., and Chang, I. D., "Heatshield Erosion in a Dusty Martian Atmosphere," *Journal of Spacecraft and Rockets*, Vol. 30, No. 2, 1993, pp. 140–151.

[30]Whiting, E. E., Arnold, J. O., Page, W. A., and Reynolds, R. M., "Composition of Earth's Atmosphere by Shock-Layer Radiometry During PAET Entry Probe Experiments," *Journal of Quantitative Spectroscopy and Radiative Transfer*, Vol. 13, No. 9, 1973, pp. 837–860.